pH Dependence and Protein Selectivity of Poly(ethyleneimine)/Poly(acrylic acid) Multilayers Studied by in Situ ATR-FTIR Spectroscopy

M. Müller,* B. Kessler, and N. Houbenov

Leibniz-Institute of Polymer Research Dresden e.V. (IPF), Hohe Strasse 6, D-01069 Dresden, Germany

K. Bohatá, Z. Pientka, and E. Brynda

Institute of Macromolecular Chemistry (IMC), Heyrovsky sq. 2, 16206 Prague 6, Czech Republic

Received August 31, 2005; Revised Manuscript Received February 10, 2006

The selective interaction between polyelectrolyte multilayers (PEM) consecutively adsorbed from poly(ethyleneimine) (PEI) and poly(acrylic acid) (PAC) and a binary mixture containing concanavalin A (COA) and lysozyme (LYZ) based on electrostatic interaction is reported. The composition and structure of the PEM and the uptake of proteins were analyzed by in situ attenuated total reflection (ATR) Fourier transform infrared (FTIR) spectroscopy, and the morphology and thickness were characterized by atomic force microscopy (AFM) and ellipsometry. The PEM dissociation degree and charge state and the protein adsorption were shown to be highly dependent on the outermost layer type and the pH in solution. High protein uptake was obtained under electrostatically attractive conditions. This was used to bind selectively one protein from a binary mixture of LYZ/COA. In detail it could be demonstrated that six-layered PEM-6 at pH = 7.3 showed a preferential sorption of positively charged LYZ, while at PEM-5 and pH = 7.3 negatively charged COA could be selectively bound. No protein sorption from the binary mixture was observed at pH = 4.0 for both PEM, when COA, LYZ, and the outermost PEI layer of PEM-5 were positively charged or the outermost PAC layer of PEM-6 was neutral. Furthermore, from factor analysis of the spectral data the higher selectivity was found for PEM-5 compared to PEM-6. Increasing the ionic strength revealed a drastic decrease in the selectivity of both PEM. Evidence was found that the proteins were predominantly bound at the surface and to a minor extent in the bulk phase of PEM. These results suggest possible working regimes and application fields of PEI/PAC multilayer assemblies related to the preparative separation of binary and multicomponent protein mixtures (biofluids, food) as well as to the design of selective protein-resistant surfaces.

Introduction

The interaction between proteins and polymer surfaces constitutes an important phenomenon in colloid and material science, where on one hand protein sorption is desired for bioactive applications (e.g., uptake of collagenized implants), and on the other it should be prevented for bioinert purposes (e.g., clotting on medical devices, membrane fouling) in order to block or delay further bioadhesion cascades. This was extensively studied by, e.g., Baier and Dutton,[1] Brash and Lyman,[2] Royce et al.,[3] Andrade and Hlady,[4] and Haynes and Norde[5] claiming important trends and preliminary rules concerning the correlation between polymer substrate structure and susceptibility to protein sorption. However, from the physicochemical viewpoint an incommensurable number of enthalpic contributions and parameters on different length scales to the always negative Gibb's energy of protein sorption ΔG_{ADS} prevails.[5] Hence, fundamental approaches try to reduce this complex process to a predominant type of interaction force.

Recently, much experimental and theoretical work has been focused on electrostatic forces between protein and charged surfaces. Experimentally those charged surfaces can be provided by single-polyelectrolyte or polyelectrolyte brush layers,[6,7] self-assembled monolayers (SAM)[8,9] with charged end groups, and polyelectrolyte multilayers (PEM).[10,11] Concerning the first type Wang and Dubin[12] studied protein binding on polyelectrolyte-treated glass and Rosenfeldt et al.[13] the protein interaction with like-charged spherical polyelectrolyte brushes. The latter claimed counterion evaporation or local pH mediated by charge regulation in the brush layer, supported by work of Biesheuvel and Wittemann,[14] as the main driving force for the observed strong protein binding. Concerning the second type, SAM mostly made of differently terminated alkylthiols, Ostuni et al.[15] reported protein (and bacteria) repelling SAM surfaces terminated with charged (zwitterionic) derivatives, Li et al.[16] studied temperature effects of protein sorption onto carboxyl-terminated SAM, and Silin et al.[17] compared nonspecific sorption of serum albumin and immunoglobulin on amino- and carboxyl-terminated with those of oligoethyleneoxide-terminated SAM. Finally protein interaction at PEM has been extensively studied by Voegel, Schaaf and co-workers,[18−22] Salloum and Schlenoff,[23] Brynda et al.,[24] Izumrudov et al.,[25] and Müller and co-workers.[26−28] Meanwhile, it is commonly accepted that PEM assemblies are well-defined platforms to study protein sorption due to fundamental aspects and to generate protein inert or binding surfaces for several applications.

In that context recently the reversible uptake and release of single proteins with different isoelectric points (IEP) on PEM composed of poly(ethyleneimine) (PEI) and poly(acrylic acid) (PAC) by electrostatic interaction, which could be switched by

* To whom correspondence should be addressed. E-mail: mamuller@ipfdd.de.

10.1021/bm050631r CCC: $33.50
Published on Web 03/25/2006

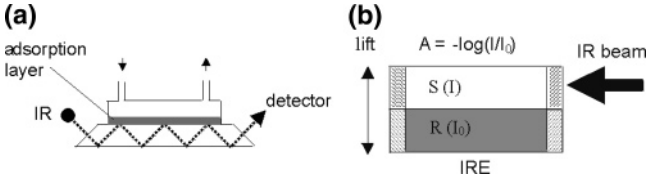

Figure 1. (a) Concept of in situ ATR-FTIR spectroscopy based on a Si IRE and sealed liquid chambers. (b) SBSR principle according to ref 34 used for reproducible spectral background compensation in in situ ATR-FTIR spectra.

the pH of the surrounding aqueous medium, was reported.[29] Exemplarily, the binding and release of the basic protein lysozyme (LYZ, IEP = 11.1) at PEM-6 and pH = 7.3 and 4.0, respectively, and of the acidic protein human serum albumin (HSA, IEP = 4.7) at PEM-7 and pH = 7.3 and 10.0, respectively, were shown. Binding was due to the charged and release due to the neutral state of the respective outermost polyelectrolyte layers. As was pointed out therein[26,30] the advantages of the PEI/PAC system consist in the convenient wet chemical preparation, the deposition reproducibility resulting in a homogeneous surface coverage, and the stability within a broad pH range and against buffer systems used for protein samples.

Since PEM have been proven so far as surface coatings, which are highly *specific* for different proteins, we were further interested if PEM are also *selective* to proteins from multicomponent mixtures, which are a more realistic model for biofluids[31] and are often encountered in biosensor and separation technology.[32] To elucidate this, we performed model studies on protein sorption from a binary mixture consisting of LYZ and concanavalin A (COA) at PEM of PEI and PAC, which to our knowledge has not been studied or reported up to now. We have chosen in situ attenuated total reflection Fourier transform infrared spectroscopy (ATR-FTIR) spectroscopy, to explore and document the sensitivity and selectivity of this surface analytical method with respect to this topic.

Experimental Section

Polyelectrolytes, Proteins. The commercial polyelectrolytes (PEL), PEI (branched, M_w = 750 000 g/mol, pH = 9; Sigma-Aldrich, Steinheim, Germany) and PAC (M_w = 50 000 g/mol, pH = 4; Polysciences Inc., Warrington, U.S.A.) were used without further purification. These PEL were dissolved in Millipore water (resistance 18.2 MΩcm) at the concentration of c_{PEL} = 0.01 M and used without any additional pH setting.

LYZ (M_w = 14 600 g/mol, IEP = 11.1) and COA (M_w = 71 000 g/mol, IEP = 5.4) were purchased from Sigma-Aldrich (Steinheim, Germany) and were used without further purification. Phosphate buffer saline (PBS, $HPO_4^{2-}/H_2PO_4^-$, 0.015 M; NaCl, 0.01 M, pH = 7.3) and citrate buffer (CB, 0.015 M, pH = 4.0) were applied as standard solvents for the protein solutions. For the PBS solutions with elevated ionic strength the NaCl concentration was changed to 0.15 M. The protein mixture was prepared by mixing the buffered solutions of 1 mg/mL LYZ and 1 mg/mL COA in the ratio of 1:1.

Surfaces. Trapezoidal silicon internal reflection elements (IRE, 50 × 20 × 2 mm^3) have been chosen. Before every experiment the IREs were cleaned by pure water (Millipore, pH = 6.5), ethanol, and chloroform followed by a plasma treatment (PCD 100, Harrick, New York) under reduced pressure.

PEM Deposition. Deposition of PEM was carried out in the in situ ATR sorption cell (Figure 1a) by consecutive sorption of cationic PEI (0.01 M) and anionic PAC (0.01 M) solutions at pH = 9 and 4, respectively, onto the silicon IRE. An automatic valve system was used. This resulted in five-layer assemblies (PEM-5) with PEI and six-layer assemblies (PEM-6) with PAC in the outermost layer, respectively. After each sorption step of PEL the sorption cell was carefully rinsed by pure water (Millipore, pH = 6.5). The duration time of sorption was 20 min, for which reproducible deposition was observed. Changes of the medium above the PEM were performed by injecting pure water, citrate, or PBS buffer in the sorption cell by syringe or by drying under a gentle N_2 stream.

Protein Sorption. Protein sorption was measured also in the in situ ATR sorption cell using PBS (pH = 7.3) or CB (pH = 4.0) solutions. Before adsorption the PEM was rinsed by the respective buffer solution. Then the buffered protein solution was injected by syringe. The duration of sorption was 2 h, followed by rinsing with the respective buffer solution. After that the sample was rinsed by pure water and dried by a gentle N_2 stream. The protein sorption data and the given errors were based on four independent series.

ATR-FTIR Spectroscopy. The principle of in situ ATR-FTIR is given in Figure 1a. The technical ATR-FTIR attachment consisted of a special mirror setup and an in situ sorption cell (IPF Dresden) operating on a commercial FTIR spectrometer (IFS 55, BRUKER Optics GmbH, Ettlingen, Germany) equipped with a globar source and MCT detector.[33] ATR-FTIR absorbance spectra were recorded by the single-beam sample reference (SBSR) method[34] (scheme in Figure 1b) based on the alternate recording of single-channel spectra of the sample half (I_S) and the reference half (I_R) of the IRE, respectively, which is also described therein.[35]

Above the sample and reference half are two sealed liquid compartments (S, R). Compartment S was filled typically either with PEL, buffer, or protein solution and compartment R with the corresponding solvent (e.g., buffer). Optionally both compartments were dried to measure samples (S) in the dry state. The resulting absorption spectra given by $A_{SBSR} = -\log(I_S/I_R)$ show convenient compensation of the background absorption and flat baselines, which is a prerequisite for quantitative ATR-FTIR spectroscopy.

ATR-FTIR Analysis. The sorbed protein amount Γ at PEM films was determined based on the effective thickness concept due to Harrick[36] and Fringeli[34] which results in the Lambert−Beer analogous equation given in eq 1

$$A_S = (N\epsilon\Gamma/d)d_e \qquad (1)$$

There, A_S is the amide I integral (1700−1600 cm^{-1}) measured with vertically (s-) polarized light ($A_S \approx 0.8$ A for isotropic layers), N is the number of active reflections, ϵ is the absorption coefficient (cm/mol), Γ is the surface concentration, which is due to mass within the projection of 1 cm^2, d is the thickness of the protein layer (cm) and the so-called effective thickness d_e (cm). d_e is given in eq 2, which is a function of the depth of penetration d_p,[36] the relative electrical field component in y-direction $E_Y = 2\cos\theta/(1 - n_{31}^2)^{1/2}$, the refractive indices of the involved media n_1 (Si), n_2 (PEM, protein), and n_3 (water), the incident angle of IR light θ, and the positions z_1 and $z_2 = z_1 + d$ denoting the start and end of the protein layer zone, respectively.

$$d_e = n_2 d_p E_Y^2/(2\cos\theta\, n_1)[\exp(-2z_1/d_p) - \exp(-2z_2/d_p)] \qquad (2)$$

Two optional concepts for the evaluation of ATR-FTIR data with respect to PEM/protein interaction may be considered, which are shown in Figure 2: protein sorption on top of the PEM (Figure 2A) and protein sorption into the bulk phase of the PEM (Figure 2B).

For the determination of Γ knowing A_S or of A_S knowing Γ the eqs 1 and 2 were combined. The A_S values (amide I) measured in the dry state (N_2 stream) after rinsing with water and the following constants and settings were used: $N = 11$, $\epsilon = 2.74 \times 10^7$ cm/mol (amide I), $n_1 = 3.50$ (Si), $n_2 = 1.45$ (polymer film, protein, dry), $n_3 = 1.00$, and $\theta = 45°$ leading to $d_p = 426$ nm. For z_1 and z_2 the thickness values determined by ellipsometry on the PEM samples in the dry state were used, which are given in Table 1.

In the case of concept A these thicknesses were used as z_1 values, and $d = z_2 - z_1$ was approximated to 50 nm, which might be not the exact value. However, having calculated the approximate Γ value of

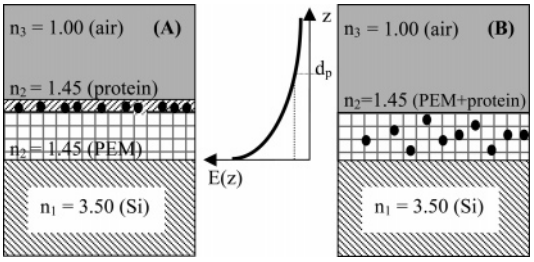

Figure 2. Two concepts (A and B) for the treatment of experimental ATR-FTIR data on protein sorption at PEM related to the course of the electrical field $E(z)$ as a function of distance z to the Si surface. (A) Protein sorption on top of the PEM: Si/PEM/protein/air. (B) Protein sorption into PEM: Si/PEM + protein/air.

the protein based on this d value, one could estimate the corresponding d value from the dimensions of the protein and set again this value into eq 1 in the sense of an iterative process. In the case of concept B these thicknesses were used as z_2 values, since $z_1 = 0$ nm.

The detection limit of the used ATR-FTIR setup with respect to the sorbed protein amount at PEM films is given by the minimum detectable amide I integral, which is around $A_{S,amidel} \approx 0.05$ cm^{-1} with respect to a convenient signal/noise ratio. On the basis of this value minimum protein surface concentrations around $\Gamma \approx 0.02$ μg/cm^2 for concept A (PEM surface) and around $\Gamma_{ATR} \approx 0.01$ μg/cm^2 for concept B (PEM bulk phase) can be calculated for both PEM-5 and PEM-6. Additionally, for comparison of the data based on H_2O solutions and rinses, D_2O was optionally used, which is advantageous, since the δ(OH) band of water is shifted from around 1640 to 1200 cm^{-1} (δ(OD)) so that the amide I band integral is not influenced in the case of insufficient spectral compensation. Moreover, upon H−D exchange the amide I band shifts to 5−10 cm^{-1} lower wavenumbers (amide I′). The amide I′ integral for adsorbed LYZ at PEM-6 was around 5% lower compared to that of the amide I integral (data not shown). Since amide I and amide I′ have around the same absorption coefficient (see below), we conclude proper compensation of the δ(OH) band in the ATR-FTIR spectra on sorbed proteins based on H_2O.

Factor Analysis of FTIR Spectra. The principle of factor analysis is mentioned in the section 4 of the Results and Discussion. For the representation of the mixed protein spectrum $A_{LYZ/COA}$ by the single-protein spectra A_{LYZ}, A_{COA} the factors of the single-protein spectra were minimized by least-squares fitting using the OPUS software (automatic subtract routine) supplied by Bruker Optics GmbH, Ettlingen, Germany. The single-protein spectra A_{LYZ} and A_{COA} were normalized due to equal amide I band integrals (1700−1600 cm^{-1}). The errors of the factors and the related resulting protein fractions are due to three independent measurements.

Atomic Force Microscopy (AFM). For the morphological AFM measurements the identical silicon IREs coated by PEM, which were studied by ATR-FTIR spectroscopy, were used. The AFM experiments were carried out with a Nanostation II from SIS GmbH (Herzogenrath, Germany) in the noncontact mode. The used tip for the experiments was a silicon probe from Nanosensors (Darmstadt, Germany) having a radius of around 10 nm according to the manufacturer. In all samples the same recording parameters, setpoint, time constant, and proportionality factor were used. As soon as artifacts appeared in the images (e.g., triangles as convolution of the tip with the object), the tip was immediately changed. AFM images are shown in the phase mode providing more contrast for these samples. In Figure 3 AFM images in the phase mode of the herein used PEM-5 and PEM-6 in the dry state are given. Although these images suggest a smoother surface morphology for PEM-5 (rms roughness, 1.06 nm) and a rough one featuring granular structures for PEM-6 (rms roughness, 13.42 nm), one has to be careful with further interpretations, since different interactions between surface and tip for the two PEM prevail. In that context long-range electrostatic attraction between the positively charged PEM-5 and negatively charged tip (Si_3N_4) might influence the non-contact mode to a higher extent compared to that of respective repulsive interactions for PEM-6 (see the Results and Discussion).

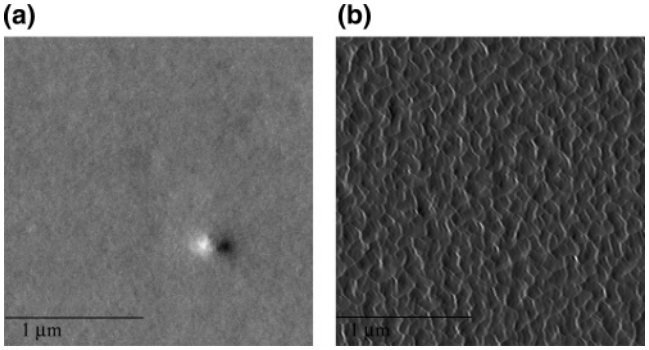

Figure 3. AFM images (phase mode, 2 × 2 μm^2) on PEM-5 (a) and PEM-6 (b) of PEI/PAC consecutively adsorbed from 0.01 M solutions (pH = 9 and 4) after rinsing with water and drying under nitrogen flow.

AFM (Nanoscope, Digital Instruments, Santa Barbara, CA) was additionally used to determine the thickness of the PEM films in the dry (30% RH) and wet state (pure water, CB). For that the PEM films were scratched carefully to the silicon bottom by a special needle or medical scalpel in the dry state. From AFM profiles the step height between the level of undamaged film and the bare silicon support at the bottom of the groove was determined. Scratches performed with equivalent pressure on the bare silicon support did not cause such profiles. The determined thickness values d_{AFM} (Table 1) were based on at least four measurements.

Ellipsometry. Null ellipsometry was applied to determine the thickness of PEM-5 and PEM-6 in the dry state. All the measurements were carried out using a Null ellipsometer (Multiscope, Optrel Berlin, Germany) in a polarizer compensator sample analyzer mode. Silicon supports were used equivalent to those applied for ATR-FTIR measurements (see above). As light source a He−Ne laser with $\lambda = 632.8$ nm was applied, and the angle of incidence was set to 70°. A multilayer model for homogeneous films covering the silicon substrate was used for calculation of the thickness of polymer layers in air, using the ellipsometric angles ψ and Δ. The refractive indexes in the calculations were $n = 3.8850$ for the silicon substrate, $n = 1.4598$ for the native silica layer, and an averaged to 1.5 refractive index for the adsorbed polymers. The thickness values d_{ELLIPS} (Table 1) are based on measurements of at least two places of at least three different samples.

Gravimetry. The mass of deposited PEM and bound protein was measured by gravimetry on a balance (Sartorius, BP 211D, Göttingen, Germany) under constant relative humidity of RH ≈ 30%. IREs coated on the front and backside within a total area of 14.6 cm^2 were used, from which surface concentrations Γ_{GRAV} (Table 1) were calculated.

Circular Dichroism (CD) Spectroscopy. A JASCO spectral polarimeter (J-810, JASCO, Gross-Umstadt, Germany) was used. CD spectra of COA and LYZ were recorded in the spectral range from 180 to 250 nm (n−π* and π−π* transition). The CD spectra were qualitatively analyzed[37,38] due to the appearance of the negative 222/208 nm doublet and the positive band at 192 nm diagnostic for the α-helical conformation and of the negative band at 217 nm characteristic for β-sheet conformation.

Results and Discussion

Herein we report on the selective interaction of PEM of PEI/PAC, with a binary protein mixture consisting of COA and LYZ. PEM of PEI/PAC were prepared according to the Decher protocol[10] by consecutive sorption from PEL solutions at silicon supports, which can be monitored quantitatively by in situ ATR-FTIR spectroscopy as was described, e.g., in ref 26. Particularly, the PEI/PAC system consecutively adsorbed at pH = 9 and pH

Table 1. Thickness, Surface Concentration, and Dissociation Degree of PEM-5 and PEM-6 after Exposure to Pure Water (H_2O), CB, PBS Buffer (PBS), and a Dry Air Stream (dry) for at Least 15 min as Measured by Ellipsometry, AFM, Gravimetry, and in Situ ATR-FTIR ($\alpha_{IR} = A_{\nu(COO^-)}/A_{PAC}$, $A_{PAC} = 1.74\ A_{\nu(C=O)} + A_{\nu(COO^-)}$ (Eq 3))

	d_{ELLIPS}	d_{AFM}	Γ_{GRAV}/ [μg/cm^2]	A_{PAC} (ATR)/ [cm^{-1}]	α_{IR}
PEM-5-dry	42 ± 10 nm	23 ± 4 nm	4.8 ± 0.7	4.00 ± 0.20	0.80
PEM-5-wet (H_2O)		35 ± 4 nm		7.01 ± 0.20	0.94
PEM-5-wet (CB)		22 ± 4 nm		7.74 ± 0.20	0.59
PEM-5-wet (PBS)				6.48 ± 0.20	0.95
PEM-6-dry	61 ± 10 nm	53 ± 6 nm	6.8 ± 0.7	8.38 ± 0.40	0.58
PEM-6-wet (H_2O)		75 ± 6 nm		13.96 ± 0.40	0.55
PEM-6-wet (CB)		66 ± 6 nm		14.95 ± 0.40	0.36
PEM-6-wet (PBS)				12.07 ± 40	0.67

= 4, respectively, was chosen, since it results in reproducible and homogeneous films. In the following PEM-5 and PEM-6 denote multilayers which were five or six times consecutively adsorbed from PEI/PAC solutions, respectively.

The paper is outlined in the following way: At first, properties of PEM-5 and PEM-6 of PEI/PAC in dependence of the buffer solution and the pH value are characterized, which forms the basis of the subsequent sections related to protein adsorption. Second, the individual properties of the two proteins LYZ and COA are introduced, and their specific sorption behavior at PEM-5 and PEM-6 in dependence of the pH value is shown. Then, on the basis of that the selective interaction of LYZ and COA from the binary mixture with PEM-5 and PEM-6 in dependence of the pH value is described, and the kinetic features of single- and mixed-protein sorption are compared. Finally, the quantitative composition of the formed protein layer at low and high ionic strength is given, and factors influencing protein selectivity of PEM are discussed.

1. Properties of PEM PEI/PAC. *1.1. Thickness.* The thickness of PEM-5 and PEM-6 was determined by in situ ellipsometry and AFM, which is summarized in Table 1.

In detail, by ellipsometry thicknesses of $d_{ELLIPS} = 42 \pm 10$ nm for PEM-5 and 61 ± 10 nm for PEM-6 were obtained in the dry state. Additionally, gravimetric measurements at the respective samples resulted in surface concentrations of $\Gamma_{GRAV} = 4.8\ \mu g/cm^2$ and 6.8 μg/cm^2, respectively. Approximating a PEM density of 1 g/cm^3, thickness values of 48 and 68 nm can be calculated, respectively, which are in good agreement to those obtained by ellipsometry within the error range. The AFM measurements were based on the depth of scratches into PEM films, which resulted in $d_{AFM} = 23 \pm 4$ nm for PEM-5 and $d = 53 \pm 5$ nm for PEM-6 in the dry state, respectively. For PEM-6 this is consistent with the ellipsometric thickness in the given error range, but for PEM-5 the AFM thickness is lower, which might be due to the undesired attractive interaction between AFM and PEM-5 in the applied tapping mode (see the Experimental Section).

When the dry and wet states (H_2O, pH = 6.5) of PEM-5 were compared, the AFM method resulted in thickness increases from 23 ± 4 nm to 35 ± 4 nm, whereas for PEM-6 a thickness increase from 53 ± 6 nm to 75 ± 6 nm was obtained. Ratioing the thickness of the wet (pure water) and dry state swelling degrees $Q = d_{WET}/d_{DRY}$ of 1.52 ± 0.1 (PEM-5) and 1.42 ± 0.1 (PEM-6) corresponding to around 50% and 40% of swelling by water uptake could be determined, respectively. Literature values are ranging between around 20% and 40% for other multilayer systems.[39−41] Kügler et al.,[39] who determined Q = 1.29 (29%) for the system poly(styrenesulfonate)/poly(allylamine) explained the unexpected low swelling degree by the high degree of entanglement of oppositely charged PEL in the bulk phase of the PEM ("quasi-neutral micelles") causing strong screening of their ionic character. This was supported by a Flory−Huggins analysis resulting in interaction parameters χ close to 1 suggesting a rather hydrophobic polymer matrix. In that context Kovacevic et al.[42] claimed the corresponding bulk phase of PEM to be in a glassy state resulting in high stability with respect to dissolution. For the outermost layer the situation was claimed to be different,[39] since incomplete screening has to be considered so that swelling might be limited to that region.

Furthermore, replacing pure water by citrate the thickness (d_{AFM}) of PEM-5 (22 ± 4 nm) and PEM-6 (66 ± 6 nm) was decreased, which will be discussed in relation to the spectroscopic results in the following section.

1.2. Molecular Composition. Further details on the interaction between PEM and buffer solutions, which is relevant for the following protein adsorption, can be obtained by in situ ATR-FTIR spectroscopy monitoring molecular changes. In Figure 4, parts a and b, ATR-FTIR spectra on PEM-5 and PEM-6 of PEI/PAC in contact to pure H_2O (bottom), PBS (pH = 7.3), and CB (pH = 4.0) solution and in the final dry state (top) are shown.

First, the spectra of PEM-5 (Figure 4a) show lower overall intensities especially in the range of 1750−1500 cm^{-1} compared to those of PEM-6, which is due to the higher thickness or deposited polymer amount of PEM-6. This is in accordance to the AFM, ellipsometric, and gravimetric data given in Table 1. In detail, the ν(C═O) and the $\nu(COO^-)$ bands at 1710 and 1555 cm^{-1} due to carboxylic acid and carboxylate groups are of great diagnostic value with respect to dissociation behavior and adsorbed amount. Both bands show a significant dependence on the pH value of the applied buffer solution, and as we outlined in previous papers (e.g., ref 33), these two bands can be used to calculate the dissociation degree α_{IR} of polycarboxylates in PEM due to the following:

$$\alpha_{IR} = A_{\nu(COO^-)}/[1.74A_{\nu(C=O)} + A_{\nu(COO^-)}] \qquad (3)$$

According to that, PEM-6 (Figure 4b) resulted in a dissociation degree of $\alpha = 0.67$ for PBS and $\alpha = 0.36$ for CB. Since ATR-FTIR is sensitive to both the bulk phase and surface region of PEM, this cannot be unambiguously attributed to the number of neutral carboxylic acid and charged carboxylate groups at the surface. However, qualitatively, a higher negative surface charge can be concluded for pH = 7.3 compared to that of pH = 4.0. For PEM-5 (Figure 4a) at pH = 7.3 a dissociation degree of $\alpha_{IR} = 0.95$ was observed, which is due to complexation (ion pairing) of underlying PAC carboxylate groups by outermost PEI ammonium groups. Surprisingly, for PEM-5 at pH = 4.0, the ν(C═O) band shows up, and $\alpha_{IR} = 0.59$ was obtained. This is a clear indication that a considerable amount of carboxylate groups in the bulk phase of the PEM were accessible to protonation and thus were not ion paired with the ammonium groups of PEI. For the PEM-5 the charge state of the outermost PEI layer cannot be characterized by IR spectroscopy like for PEM-6. Only the presence of a broad band between 3000 and 2000 cm^{-1} assigned to $\nu(NH_xR_y^+)$ moieties gives a qualitative hint for quartenized ammonium groups of PEI. This band is intense at pH = 4 (citrate) and is still present but slightly weakened at pH = 7.3 (PBS) indicative for positive surface charge. Conclusively, in Table 2 the expected charge properties of PEM-5 and PEM-6 in dependence of the pH value are summarized.

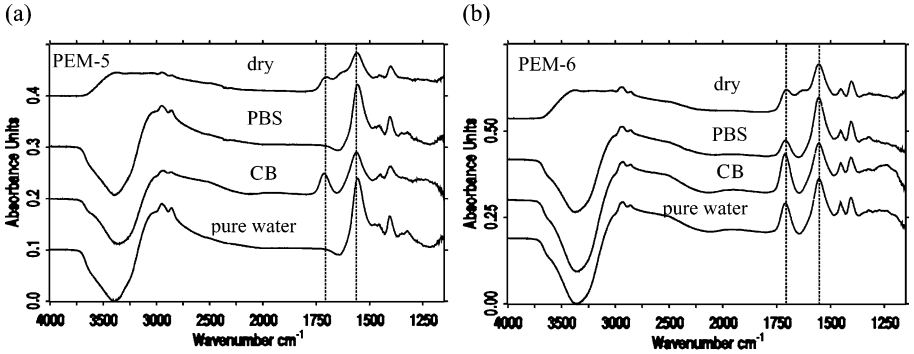

Figure 4. ATR-FTIR spectra on the PEM-5 (a) and PEM-6 (b) of PEI/PAC in pure water, at pH = 4 (citrate) and 7.3 (PBS) and in the dry state (from bottom to top), respectively.

Table 2. Physicochemical Properties of LYZ and COA

	LYZ	COA
mol wt [g/mol][a]	14 600	71 000
IEP[b]	11.1	5.4
conformation (X-ray structure)[c]	46% α-helix	3% α-helix
	19% β-sheet	65% β-sheet
	23% β-turn	22% β-turn

[a] Ref 44. [b] Ref 44. [c] Refs 45 and 46.

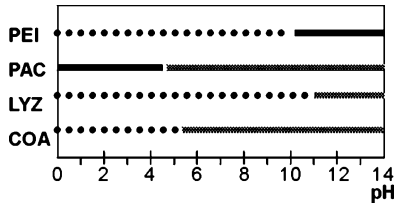

Figure 5. Influence of the pH value on the charge states of the outermost PEI or PAC layer and of the proteins LYZ and COA based on IEP and protonation behavior given in refs 44, 47, and 48. The black dots represent the pH range for positive, the gray line for negative, and the black line for no charge.

Moreover, the denominator of eq 3, $A_{PAC} = 1.74A_{\nu(C=O)} + A_{\nu(COO^-)}$, can be used as a relative measure of concentration within PEM films in contact to pure water, PBS, and CB, which is shown in Table 1. In detail, for PEM-5 CB revealed the largest A_{PAC} value (7.74 cm^{-1}), while pure water (7.01 cm^{-1}) and PBS buffer (6.48 cm^{-1}) showed lower ones. For PEM-6 the absolute A_{PAC} values were larger (citrate, 14.95; pure water, 13.96; PBS, 12.07 cm^{-1}) compared to those of PEM-5, which is due to the additional PAC layer of PEM-6. Moreover, the trend of the pH dependence was similar to PEM-5 from citrate, pure water to PBS buffer. Generally, in the thin film case absorbance variations (e.g., A_{PAC}) can result from four contributions: changes of the density (i), thickness (ii), and refractive index (iii), e.g., by deswelling/swelling or of the adsorbed amount (iv).[36,43] Since the adsorbed amount cannot increase and density and thickness are in a first approximation complementary, obviously, the increased A_{PAC} values for PEM-5 and PEM-6 under CB are due to an increase in the refractive index. This can be explained by the higher coiled state of the lower dissociated and charged PAC component, which results in a less hydrated and compact bulk phase of the PEM. This is qualitatively supported by the decreased AFM thicknesses of PEM-5 and PEM-6 for CB in comparison to that of pure water (Table 1). Additionally, the uptake of citrate into the PEM might also contribute to the A_{PAC} value due to its carboxyl bands.

In contrast for PEM-5 and PEM-6 under PBS buffer from the lower A_{PAC} values a decrease of adsorbed amount (iv) or of the refractive index (iii) could be considered. The former would suggest a small loss of around 10% with respect to PEM in contact to pure water. The latter could be due to the higher dissociation and charge density of PAC, which leads on one hand to a more extended conformation and on the other to a more hydrated bulk phase of the PEM. Presumably both contributions are partly valid, and additionally it could be speculated on uptake of the phosphate ions into the PEM, which causes swelling of the polymer phase.

No absorbance changes could be specifically attributed to the PEI component so that these conclusions on structural changes in the PEM are limited to the PAC component. However, the pH changes from 4.0 to 7.3 should not influence PEI charge density and conformation as significantly as that of PAC so that concentration changes are mainly related to PAC.

Summarizing the characterization experiments PEM films show moderate swelling from the dry to the wet state and no large thickness variations upon changing the aqueous media. From this a rather dense structure of PEM and the possibility to compare directly adsorbed protein amounts in dependence of the pH value can be concluded. No direct conclusions can be drawn with respect to porosity of PEM relevant for the protein sorption mechanism.

2. Protein Sorption at PEM from a Single-Component Solution. *2.1. Sorbed Amount.* For the studies on the interaction between PEM and proteins from single- or two-component solutions PEM the model proteins LYZ, which is a carbohydrate-digesting protein, and COA, which is a carbohydrate-binding protein (lectin), were chosen. They are establishing different properties due to their molecular weight (M_w), IEP, and conformation, as summarized in Table 2.

Especially important with respect to protein sorption at charged interfaces is the protein IEP, which is determined by the ratio of the basic (Lys, Arg, His), to acidic (Glu, Asp) amino acid residues. Concerning that LYZ establishes at both applied values of pH = 7.3 and pH = 4.0 a positive net charge, while COA at pH = 7.3 is negatively and at pH = 4.0 is positively charged. The charge ranges of the two proteins in dependence of the pH are given and compared to those of PEM-5 and PEM-6 in Figure 5.

In Figure 6 ATR-FTIR difference spectra reflecting interaction of LYZ at PEM-6 (upper spectrum) and of COA at PEM-5 (lower spectrum) both sorbed for 120 min and rinsed at pH = 7.3 (PBS buffer) are shown. No negative peaks due to ν(C═O) and $\nu(COO^-)$ bands were visible in both spectra, which is a proof for film stability upon protein adsorption. For both proteins intense amide I and II signals were obtained in the wavenumber range between 1700 and 1500 cm^{-1}, which is a qualitative measure for strong interaction to PEM. Qualitatively, this can be explained, that at pH = 7.3 LYZ and COA were adsorbed

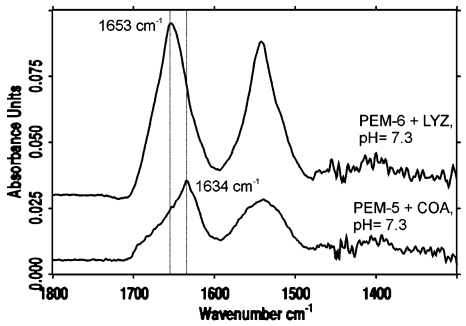

Figure 6. ATR-FTIR difference spectra between PEM-6 after contact to buffered LYZ solution and rinsing and PEM-6 in contact to PBS buffer (upper spectrum) and between PEM-5 after contact to COA solution and rinsing and PEM-5 in contact to PBS buffer (lower spectrum) both sorbed and rinsed at pH = 7.3 (concentration of PBS and protein, 1 mg/mL).

Table 3. Surface Concentrations of LYZ and COA at PEM in the Dry State Obtained by ATR-FTIR Spectroscopy (Γ_{ATR}) According to Concepts A and B Using Eq 1 and the Corresponding Thickness Values of Table 1 (z_1 = 61 nm (PEM-6), z_1 = 42 nm (PEM-5)) and by Gravimetry (Γ_{GRAV})

sample	A/[cm^{-1}]	Γ_{ATR}/[μg/cm^2] concept A	Γ_{ATR}/[μg/cm^2] concept B	Γ_{GRAV}/[μg/cm^2][a]
PEM-6 + LYZ	2.82 ± 0.20	1.15 ± 0.10	0.88 ± 0.10	2.05 ± 0.50
PEM-5 + COA	0.77 ± 0.10	0.28 ± 0.03	0.23 ± 0.03	0.68 ± 0.20
PEM-6 + LYZ/COA	3.07 ± 0.20	1.25 ± 0.10	0.96 ± 0.10	
PEM-5 + LYZ/COA	1.14 ± 0.10	0.43 ± 0.03	0.34 ± 0.03	

[a] The large error is due to different water uptake of bare and protein-bound PEM.

by electrostatic attraction at the respective oppositely charged surface of PEM-6 (negative) and PEM-5 (positive), as described in the preceding section.

However, quantitatively these experimental values can be analyzed due to two different concepts of PEM/protein interaction with respect to protein location, as was mentioned in the Experimental Section: adsorption at the surface of the PEM (concept A) or sorption into the PEM bulk phase (concept B). To elucidate which concept is the more valid, surface concentrations of both proteins after interaction with their respective PEM were calculated for the dry state according to eq 1 (see the Experimental Section) for both concepts and were compared with gravimetric measurements on the bound protein in the dry state, which is summarized in Table 3. Obviously, concept B resulted in lower (0.88 and 0.23 μg/cm^2) and concept A in higher Γ_{ATR} values (1.15 and 0.28 μg/cm^2) for LYZ at PEM-6 and COA at PEM-5, respectively. Taking into account that dry PEM may contain at least around 20% (w/w) of water under ambient conditions,[41] the corrected surface concentrations obtained by gravimetry (1.64 and 0.54 μg/cm^2, respectively, scaled from values of Table 1) are closer to those determined by concept A so that a certain priority of the surface adsorption process is considered. However taking into account that the Γ_{ATR} values found by concepts A and B are not that much deviating, also a considerable degree of migration into the PEM might take place, which was claimed by Salloum and Schlenoff[23] and Szyk et al.[19] Presumably, after an initial adsorption step of proteins at the oppositely charged surface, migration of the surface-bound protein into the bulk phase of the PEM (absorption) is possible. However, the hydrophobic and neutral nature of the PEM bulk phase, claimed by Kügler et al.[39] and Kovacevic et al.,[42] limits a higher uptake of proteins. Furthermore, based on a PEM model claiming a core zone of 1:1 stoichiometry and an outer zone of excess charge,[49] we speculate that proteins predominantly interact with the loose PEM outer zone (1−2 outermost layers) but do not penetrate further.

Regardless of the mechanism (A or B) the Γ values found by ATR-FTIR and gravimetry given in Table 3 are indicative of high protein binding, which is in the lines of previously reported work.[26,28] Concerning the total protein uptake COA was bound to PEM-5 around 4 times less than LYZ to PEM-6 (Table 3). This can be explained considering various factors. At first both proteins have different IEPs resulting in differently scaled electrostatic attraction: LYZ is stronger sorbed compared to COA, since according to Table 2 the IEP of LYZ differs by around 4 and that of COA only by around 2 pH units from the applied pH of 7.3. This dependence on the magnitude |IEP − pH| was already shown for other proteins at comparable systems therein.[28] Second, LYZ is smaller than COA and might be better incorporated due to sterical aspects at the rough outermost PEM zone.

At pH = 4.0 no protein sorption within the limit of ATR-FTIR detection, neither of COA at PEM-6 nor of LYZ at PEM-5 was observed (data not shown). This is due to electrostatic repulsion of negatively charged COA and positively charged LYZ at their respective like-charged PEM, which is illustrated in Figure 5.

2.2. Protein Conformation. Inspecting the spectra of attractively sorbed LYZ and COA, which are shown in Figure 6, a significant variation of the line shape and the position of the amide I band maximum can be realized. In detail the LYZ spectrum shows an amide I band maximum at 1653 cm^{-1}, and the COA spectrum shows one at 1634 cm^{-1}. It is well-known that infrared spectroscopy is highly sensitive to the conformation of proteins and that the wavenumber maximum and the line shape of the amide I band correlate with the secondary structure of a given protein. This concept was initiated by early observations of Elliott and Ambrose[50] at casted polypeptide films and was subsequently developed and applied by various authors to natural proteins in the following time (e.g., ref 51). As a result correlations between amide line shape and conformation of proteins are valid, which at least may serve for qualitative assignments of dissolved or sorbed proteins. Concerning these assignments[51] (and further references therein) the amide I peak for proteins containing predominantly α-helical structure appears in the range of 1648−1660 cm^{-1} and for proteins with predominant β-sheet structure in the range of 1625−1635 cm^{-1}. Additionally, the protein conformation of LYZ and COA was checked by CD spectroscopy, which qualitatively resulted in significant differences (data not shown): the LYZ CD spectrum showed the doublet at 220 and 208 nm indicative for α-helical structures, and that of COA showed a positive signal around 195 nm and a negative one around 222 nm, which could be assigned to β-turn and β-sheet structures, according to theoretical calculations of Woody.[52,53] Moreover, both findings are consistent with the X-ray data on LYZ and COA conformation in the solid state given in Table 2. Conclusively, the obvious difference between the ATR-FTIR spectra of both proteins correlates with results of other techniques and hence could be used for the discrimination of both proteins, which will be shown in section 3.

2.3. Morphology. In Figure 7 AFM images on PEM-5 (Figure 7a) and PEM-6 (Figure 7b) after adsorption of COA and LYZ, respectively, in the dry state are shown, which have to be compared with those for both PEM before adsorption (Figure 3, parts a and b).

Surprisingly, for PEM-5 the smooth and featureless morphology in the AFM image before adsorption (Figure 3a; rms

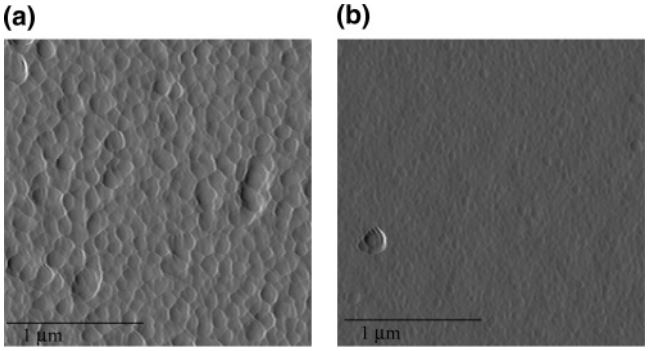

Figure 7. AFM images (phase mode, 2 × 2 μm^2) on PEM-5 (a) and PEM-6 (b) of PEI/PAC after sorption of COA and LYZ, respectively (dry state after rinsing).

roughness, 1.06) changed after COA adsorption, and granular structures were visible (rms roughness, 10.51 nm). In contrast, for PEM-6 the granular structures before (Figure 3b; rms roughness, 13.42) vanished after LYZ adsorption, and a smooth morphology showed up (rms roughness, 5.04 nm). As we pointed out in the Experimental Section the lack of structure in the PEM-5 micrograph might be due to attractive tip/surface interaction. Presumably, after adsorption of COA the positive surface charge of PEM-5 changed to a negative one, allowing for AFM imaging with appropriate resolution of structural details. In contrast, after adsorption of LYZ the negative surface charge of PEM-6 changed to a positive one resulting in lower resolution of the true surface structure. From these findings we conclude formation of protein films on top of both PEM, which are able to reverse the surface charge of the bare PEM surface. This supports our conclusion from ATR-FTIR analysis and gravimetry that, besides a minor amount of protein migrated into the bulk phase of the PEM, a major part is surface bound, which was already discussed by other authors.[19,23]

3. Protein Sorption at PEM from a Binary Mixture. In the preceding section we have reported the specific sorption of LYZ and COA from their single-component solutions at the oppositely charged PEM, and evidence was found that the proteins are bound to a major degree at the surface region and a minor one in the bulk phase. Thereupon, we were further interested from both analytical and preparative aspects in the selective sorption of one of those proteins from a binary mixture at PEM. The question was whether PEM of PEI/PAC are able to discriminate or separate one of the two proteins from their mixture and if ATR-FTIR spectroscopy is a convenient analytical tool for that. At that point it has to be noted that mixing COA and LYZ under pH conditions, where the two proteins were oppositely charged, did not result in turbid dispersions or phase separation by complexation, which is a prerequisite for this experiment. We explain this by the ampholytic nature of proteins allowing for LYZ and COA besides globally attractive also locally repulsive electrostatic interaction. As substrates again PEM-5 and PEM-6 of PEI/PAC were used, and the LYZ/COA mixture was sorbed at pH = 4.0 and pH = 7.3, followed by a respective buffer rinse.

3.1. Interaction of the Binary Protein Mixture with PEM-5. In Figure 8 ATR-FTIR difference spectra, reflecting the bound protein at PEM-5 after contact to a buffered LYZ/COA mixture followed by rinsing for pH = 4 (lower curve) and pH = 7.3 (upper curve), are shown.

Significantly, for pH = 7.3 an intense amide I band due to protein sorption from the binary mixture at PEM-5 was obtained. When this spectrum, whose amide I peak maximum appeared at 1633 cm^{-1}, is compared with the respective individual spectra

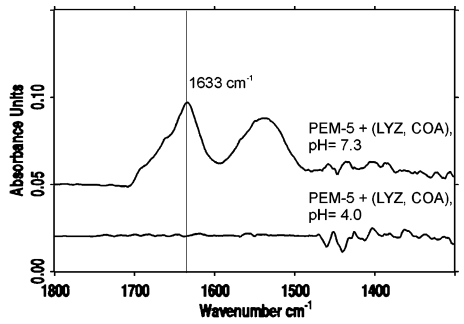

Figure 8. ATR-FTIR difference spectra on the interaction of a mixture of LYZ and COA (1 mg/mL) at pH = 7.3 (upper curve) and at pH = 4.0 with the PEM-5 of PEI/PAC.

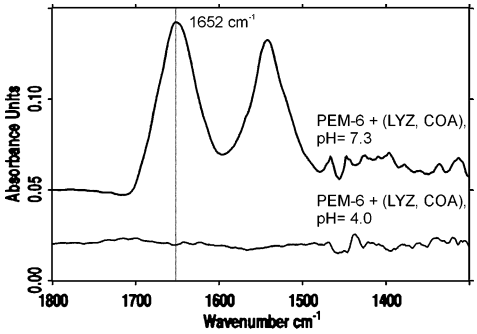

Figure 9. ATR-FTIR difference spectra on the interaction of a mixture of LYZ and COA (1 mg/mL) at pH = 7.3 (upper curve) and at pH = 4.0 with the PEM-6 of PEI/PAC.

of LYZ and COA shown in Figure 6, a similarity with the spectrum of COA (lower spectrum) can be obtained. From this qualitatively a predominant sorption of COA from the binary mixture was concluded. Analogously to the quantification concept of single-protein uptake for the binary protein mixture a protein surface concentration of around 0.43 μg/cm^2 (Table 3) at PEM-5 was calculated. The selective high uptake of COA at PEM-5 was caused by electrostatic interaction so that negatively charged COA was taken up by the PEM with positively charged surface region.

For pH = 4.0 a straight line in the wavenumber region between 1800 and 1300 cm^{-1} was obtained. On the basis of the ATR-FTIR detection limit given in the Experimental Section a maximum protein surface concentration of $\Gamma \approx 0.02$ μg/cm^2 for pH = 4.0 has to be considered, which is small compared to the value obtained for pH = 7.3. Under this condition all involved compounds COA, LYZ, and the outermost PEI layer are positively charged, which can be rationalized in Figure 5, resulting in low binding due to electrostatic repulsion of both proteins at PEM-5.

3.2. Interaction of the Binary Protein Mixture with PEM-6. Figure 9 shows ATR-FTIR difference spectra reflecting the bound protein at PEM-6 after contact to a buffered LYZ/COA mixture followed by rinsing for pH = 4 (lower curve) and pH = 7.3 (upper curve). In the spectrum taken at pH = 7.3 an intense amide I band, whose wavenumber position at 1652 cm^{-1} was similar to that of the individually sorbed LYZ shown in Figure 6 (upper spectrum), was observed. Hence, for this pH value we concluded preferential sorption of LYZ from the binary mixture at the PEM-6, which is due to the selective electrostatic attraction between outermost polyanion-rich region and LYZ and repulsion of COA. Quantitatively, a protein surface concentration of 1.25 μg/cm^2 was calculated (Table 3). This is around 3 times higher compared to the sorption from the protein mixture at PEM-5, which, like for the single-protein sorption,

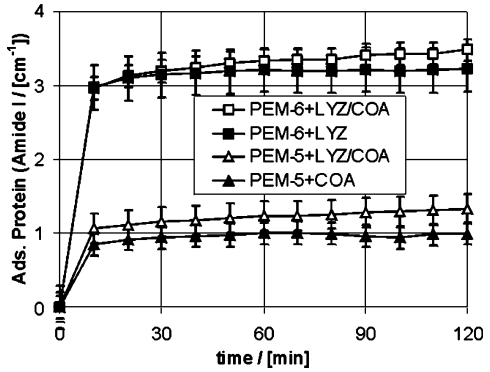

Figure 10. Sorption kinetics from single-protein solutions (LYZ, COA) and from their binary mixture (LYZ/COA) at PEM-5 and PEM-6 (pH = 7.3), respectively.

might be due to the higher magnitude of the LYZ charge (IEP = 11.1) at pH = 7.3 compared to that of COA (IEP = 5.4). No amide I intensity was detected for PEM-6 at pH = 4.0, from which again a low sorbed amount was concluded. In that case both proteins are positively charged, and the PAC in the outermost region is neutralized to a high extent, which prevents electrostatic attraction between proteins and PEM-6.

3.3. Sorption Kinetics. In Figure 10 the sorption kinetics of the single proteins (COA, LYZ) and of the binary mixture (LYZ/COA) from their solutions at PEM-5 and PEM-6, which all were related to attractive interaction between PEM and protein, are given.

In detail, the integrated amide I band areas recorded during sorption of COA and of LYZ/COA at PEM-5 and of LYZ and LYZ/COA at PEM-6 at pH = 7.3, respectively, are shown in dependence of time. All four courses show comparable kinetic features: after an initial rise an additional long-term drift was observed. An analytical description of these time courses is not straightforward, since besides the low time resolution we have to consider overlapping adsorption and absorption (diffusion) processes in the PEM/protein interaction. This is even more complicated in the case of the protein mixture, where two different proteins contribute. Nevertheless, we tried to simulate these time courses $A(t)$ empirically by the sum of two exponentially damped functions:

$$A(t) = A_1(1 - \exp(-k_1 t)) + A_2(1 - \exp(-k_2 t)) \quad (4)$$

This resulted in time constants of around $k_1 = 0.45 \pm 0.10$ min^{-1} and $k_2 \approx 0.01-0.07$ min^{-1} for both single- and mixed-protein adsorption, whereby the fast process was the predominant one ($\approx$75−90%). The occurrence of two processes might be attributed to the combined adsorption and absorption mechanism, which was already discussed above with respect to the appropriate quantification concept for the ATR-FTIR data. This result supports qualitatively the assumption that the adsorbed proteins are located on top of the PEM rather than in the PEM bulk phase. Hence, selectivity to one of the proteins of the mixture is established by the outermost PEL layer zone.

4. Quantitative Analysis of Protein Composition. To address selectivity properties of the studied PEM system more quantitatively, factor analysis[54] of protein IR spectra was applied providing for the composition of the protein layer, sorbed from the binary mixture at PEM-5 and PEM-6. A similar approach to determine the composition of plasma protein layers sorbed at bare or polymer-coated germanium supports was reported by Chittur et al. therein.[55] The concept of factor analysis[54] is principally based on the linear combination of the spectra of purely sorbed LYZ (A_{LYZ}) and COA (A_{COA}) given in Figure 6, by which the spectrum of the protein layer sorbed from the protein mixture ($A_{LYZ/COA}$) at PEM-5 (Figure 8, top) and that for PEM-6 (Figure 9, top), respectively, with unknown composition can be represented. This was done under the assumption that there is no conformational difference between the proteins, which are sorbed from the single- compared to the mixed-component solution. The following analytical eq 5 was used, and the unknown factors a and b were optimized by least-squares minimization:

$$A_{LYZ/COA} = aA_{LYZ} + bA_{COA} \quad (5)$$

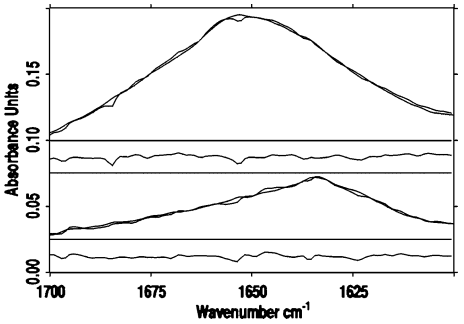

Figure 11. Factor analysis results on the ATR-FTIR spectra of the protein layer sorbed from the binary mixture (low ionic strength) at PEM-5 (bottom) and PEM-6 (top) using eq 5. The experimental, simulated, and the difference (residuals) ATR-FTIR spectra are shown.

Table 4. Relative Fractions $a/(a + b)$ of LYZ and $b/(a + b)$ of COA in the Final Protein Layer Adsorbed from the Binary Mixture at PEM-5 and PEM-6 for Low and High Salt Concentration c_S of NaCl

	LYZ/[%]	COA/[%]
PEM-5 + COA, 0.01 M		100
PEM-6 + LYZ, 0.01 M	100	
PEM-5 + LYZ/COA, 0.01 M	5 ± 5	95 ± 5
PEM-6 + LYZ/COA, 0.01 M	82 ± 5	18 ± 5
PEM-5 + LYZ/COA, 0.15 M	41 ± 10[a]	59 ± 10[a]
PEM-6 + LYZ/COA, 0.15 M	31 ± 10[a]	69 ± 10[a]

[a] The larger errors for the protein fractions at high c_S are due to the smaller amide I signals.

The result is shown in Figure 11 for the ATR-FTIR spectra of LYZ/COA mixture at PEM-5 (lower curves) and PEM-6 (upper curves), where the experimental, the simulated, and the difference between both spectra (residuals) are given. From $a/(a + b)$ the relative fraction (in percentage) of sorbed COA and from $b/(a + b)$ that of LYZ in the mixed protein layer can be obtained. According to that for the LYZ/COA mixture in contact to PEM-5 and at pH = 7.3 a composition of 95 ± 5% COA and 5 ± 5% LYZ in the sorbed protein layer was obtained. For the LYZ/COA mixture at the PEM-6 and pH = 7.3 fractions of 82 ± 5% LYZ and 18 ± 5% COA were determined, which is summarized in Table 4. Hence, in the given range of error at the PEM-5 the protein layer consisted practically exclusively of COA, whereas at the PEM-6 besides the major fraction of LYZ also a considerable minor fraction of COA was found. Since for the single-protein sorption at the PEM-6 under repulsive conditions no COA sorption was obtained (data not shown), we speculate that COA could have been cosorbed at an already preformed layer of LYZ. However, vice versa this was not observed for LYZ/COA at the PEM-5, characterizing the PEM-5 as having higher selectivity to separate one of the proteins from the other compared to PEM-6.

A possible explanation for cosorption is based on the following scenario: in a rapid first step COA and LYZ bind selectively from the protein mixture with their oppositely charged patches (majority) at PEM-5 and PEM-6, respectively, exposing their cationic (COA) or anionic (LYZ) patches (minority), respectively. Second, the respective other protein in solution is like charged to this protein layer but might be attracted also by its oppositely charged patches (minority). Presumably, this subprocess is again influenced by the different magnitudes |IEP − pH| for COA (≈2) and LYZ (≈4) in solution, which might cause stronger binding of COA (weaker opposing net charge) at the preformed LYZ layer (PEM-6) compared to that of LYZ (stronger opposing net charge) at the preformed COA layer (PEM-5). Additional driving forces might be dispersive forces between COA and LYZ.

4.1. Effect of Ionic Strength on Protein Selectivity. Having pointed out that sorption and selectivity performance of PEM are due to electrostatic interaction, we finally studied the effect of ionic strength. For that the NaCl concentration in the PBS buffer was changed from c_S = 0.01 M to 0.15 M, which corresponds to physiological salt conditions (0.9% NaCl). The protein sorption experiments, quantification as well as the factor analysis, were carried out in analogy to those with low salt. First of all the adsorbed amounts decreased drastically to around 30% for the high compared to the low ionic strength (data not shown), which is due to the decreased Debye length. Second, for the high ionic strength the fractions of the preferentially sorbed proteins decreased from 95% to 59% (COA) for PEM-5 and from 82% to 31% (LYZ) for PEM-6, as shown in Table 4. This drastic selectivity drop for both PEM at high ionic strength can be explained by an enhanced tendency for cosorption of the respective other protein. The interplay of driving forces for this cosorption is complex, among which the increased dispersive interaction between proteins in solution and either the preformed protein layer or the bare PEM have to be mainly considered. Additionally, salt screening influences significantly the mechanism of charged patches interaction, mentioned above, as outlined in a recent paper for native and succinylated (negatively charged) LYZ sorbed on silica by Biesheuvel et al.[56] so that charged protein patches prevailing for high Debye lengths are not affecting anymore for low ones (high ionic strength). Molecular modeling of the exposed surface areas of the presorbed protein with respect to charged and hydrophobic amino acids shall give deeper insight.

Conclusion

This work demonstrates for the first time that PEM can be successfully used for the selective binding of proteins from a binary mixture based on electrostatic interaction. Selective protein sorption on PEM was controlled by the outermost PEL of the PEM and by the pH of the solution. The analytical potential of quantitative ATR-FTIR spectroscopy with respect to the detection of pH-induced structural changes and charge state in PEM and of protein sorption was shown and supported by AFM and ellipsometry.

Surface and layer characterization by ATR-FTIR, AFM, and ellipsometry evidenced stable PEM films, which show moderate swelling between dry and wet states and upon changes of the surrounding aqueous media (pure water, PBS, CB).

ATR-FTIR protein binding data was evaluated by two concepts confirming protein adsorption at the outermost layer as the major process and uptake into the bulk phase of PEM as the minor, which was supported by gravimetry and AFM data.

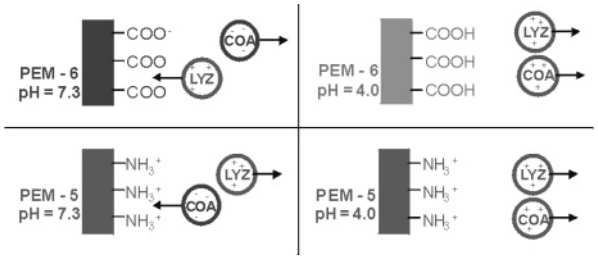

Figure 12. Proposed scheme of the selective sorption of LYZ and COA from the binary protein mixture at low ionic strength (0.01 M NaCl) at PEM-5 and PEM-6 of PEI/PAC.

Selectivity of protein sorption at PEM provided by the correlation between amide band position and protein secondary structure was outlined for the first time. This was shown for a binary mixture of LYZ and COA and the PEM system of PEI/PAC terminated either by PEI (PEM-5) or PAC (PEM-6), which is summarized in Figure 12. Predominant sorption of LYZ from the binary mixture was obtained at PEM-6 and pH = 7.3, for which LYZ was positively and PAC in the outermost zone negatively charged, while like-charged COA was not sorbed. Negatively charged COA could be selectively sorbed from the binary mixture for pH = 7.3 at PEM-5, exposing positively charged PEI, while like-charged LYZ was repelled. At pH = 4 no protein adsorption was observed for both PEM, since both proteins and the surface zone of PEM-5 were positively charged, whereas the surface zone of PEM-6 was neutral.

From factor analysis of the spectral data the higher selectivity and separation performance was found for PEM-5, which exclusively sorbed COA and rejected LYZ, in comparison to PEM-6, on which besides a major fraction of LYZ a small amount of COA was cosorbed. Increasing ionic strength to physiological conditions revealed a drastic decrease in the selectivity of both PEM. This limits in situ applications in natural biofluids such as blood and confines working regimes for those related to separation technology.

Further PEM systems offering additional discriminating interaction forces as well as multicomponent protein mixtures will be studied in future work to address selective protein-resistant surfaces, novel materials for protein separation from complex biofluids, and the analytical limits of ATR-FTIR spectroscopy in that respect. Although the introduced analytical concept will not compete with or replace fluorescence/isotope labeling or immunochemical techniques, it offers advantages with respect to versatility and availability.

Acknowledgment. We thank the Deutsche Forschungsgemeinschaft (DFG) for financial support (SFB 287, B5, EGC 720).

References and Notes

(1) Baier, R. E.; Dutton, R. C. *J. Biomed. Mater. Res.* **1969**, *3*, 191−206.
(2) Brash, J. L.; Lyman, D. J. *J. Biomed. Mater. Res.* **1969**, *3*, 175−189.
(3) Royce, F. M.; Ratner, B. D.; Horbett, T. A. Advances in Chemistry Series 199; American Chemical Society: Washington, DC, 1982; pp 453−462.
(4) Andrade, J. D.; Hlady, V. *Adv. Polym. Sci.* **1986**, *79*, 1−63.
(5) Haynes, C. A.; Norde, W. *Colloids Surf., B* **1994**, *2*, 517.
(6) Halperin, A.; Tirrel, A.; Lodge, T. P. *Adv. Polym. Sci.* **1992**, *100*, 31.
(7) Rühe, J.; Yano, R.; Lee, J. S.; Köberler, P.; Knoll, W.; Offenhäuser, A. *J. Biomater. Sci. Polym. Ed.* **1999**, *10*, 859.
(8) Sagiv, J. *J. Am. Chem. Soc.* **1980**, *102*, 92.
(9) Ulman, A. *Chem. Rev.* **1996**, *96*, 1533.

(10) Decher, G.; Hong, J. D.; Schmitt, J. *Thin Solid Films* **1992**, *210/211*, 831.
(11) Decher, G. *Science* **1997**, *277*, 1232.
(12) Wang, Y.; Dubin, P. L. *J. Chromatogr., A* **1998**, *808* (1−2), 61−70.
(13) Rosenfeldt, S.; Wittemann, A.; Ballauff, M.; Breininger, E.; Bolze, J.; Dingenouts, N. *Phys. Rev. E: Stat., Nonlinear, Soft Matter Phys.* **2004**, *70*, 61403.
(14) Biesheuvel, P. M.; Wittemann, A. *J. Phys. Chem. B* **2005**, *109* (9), 4209−4214.
(15) Ostuni, E.; Chapman, R. G.; Liang, M. N.; Meluleni, G.; Pier, G.; Ingber, D. E.; Whitesides, G. M. *Langmuir* **2001**, *17* (20), 6336−6343.
(16) Li, L.; Chen, S.; Jiang, S. *Langmuir* **2003**, *19* (7), 2974−2982.
(17) Silin, V. V.; Weetall, H.; Vanderah, D. J. *J. Colloid Interface Sci.* **1997**, *185* (1), 94−103.
(18) Ladam, G.; Gergely, C.; Senger, B.; Decher, G.; Voegel, J. C.; Schaaf, P.; Cuisinier, F. J. *Biomacromolecules* **2000**, *1* (4), 674−87.
(19) Szyk, L.; Schaaf, P.; Gergely, C.; Voegel, J. C.; Tinland, B. *Langmuir* **2001**, *17* (20), 6248−6253.
(20) Ladam, G.; Schaaf, P.; Decher, G.; Voegel, J. C.; Cuisinier, F. J. *Biomol. Eng.* **2002**, *9* (2−6), 273−80.
(21) Schwinte, P.; Ball, V.; Szalontai, B.; Haikel, Y.; Voegel, J. C.; Schaaf, P. *Biomacromolecules* **2002**, *3* (6), 1135−43.
(22) Gergely, C.; Bahi, S.; Szalontai, B.; Flores, H.; Schaaf, P.; Voegel, J. C.; Cuisinier, F. J. G. *Langmuir* **2004**, *20* (13), 5575−5582.
(23) Salloum, D. S.; Schlenoff, J. B. *Biomacromolecules* **2004**, *5* (3), 1089−96.
(24) Brynda, E.; Houska, M.; Jiroušková, M.; Dyr, J. E. *J. Biomed. Mater. Res.* **2000**, *51*, 249−257.
(25) Izumrudov, V. A.; Kharlampieva, E.; Sukhishvili, S. A. *Biomacromolecules* **2005**, *6* (3) 1782−1788.
(26) Müller, M.; Rieser, T.; Lunkwitz, K.; Berwald, S.; Meier-Haack, J.; Jehnichen, D. *Macromol. Rapid Commun.* **1998**, *19* (7), 333.
(27) Müller, M.; Briššová, M.; Rieser, T.; Powers, A. C.; Lunkwitz, K. *Mat. Sci. Eng. C.* **1999**, *8*−*9*, 167.
(28) Müller, M.; Rieser, T.; Dubin, P.; Lunkwitz, K. *Macromol. Rapid Commun.* **2001**, *22*, 390.
(29) Müller, M.; Kessler, B.; Adler, H.-J.; Lunkwitz, K. *Macromol. Symp.* **2004**, *210*, 157−164.
(30) Müller, M.; Meier-Haack, J.; Schwarz, S.; Buchhammer, H. M.; Eichhorn, K. J.; Janke, A.; Kessler, B.; Nagel, J.; Oelmann, M.; Reihs, T.; Lunkwitz, K. *J. Adhes.* **2004**, *80*, 521.
(31) Lu, C. F.; Nadarajah, A.; Chittur, K. K. *J. Colloid Interface Sci.* **1994**, *168*, 152−161.
(32) Wisniewski, N.; Reichert, M. *Colloids Surf., B* **2000**, *18*, 197−219.
(33) Müller, M. In *Handbook of Polyelectrolytes and Their Applications*; Tripathy, S. K., Kumar, J., Nalwa, H. S., Eds.; American Scientific Publishers: Stevenson Ranch, CA, 2002; Vol. 1, p 293.
(34) Fringeli, U. P. In *Encyclopedia of Spectroscopy and Spectrometry*; Lindon, J. C., Tranter, G. E., Holmes, J. L., Eds.; Academic Press: San Diego, CA, 2000.
(35) Müller, M.; Rieser, T.; Lunkwitz, K.; Meier-Haack, J. *Macromol. Rapid. Commun.* **1999**, *20*, 607.
(36) Harrrick, N. J. *Internal Reflection Spectroscopy*; Harrick Sci. Corp.: Ossining, New York, 1979.
(37) Greenfield, N.; Fasman, G. D. *Biochemistry* **1969**, *8* (10), 4108−4116.
(38) Woody, R. W. In *Circular Dichroism: Principles and Applications*; Nakanishi, K., Berova, N., Eds.; VCH Publisher: Weinheim, Germany, 1994; pp 473−483.
(39) Kügler, R.; Schmitt, J.; Knoll, W. *Macromol. Chem. Phys.* **2002**, *203*, 413−419.
(40) Sukhorukov, G. B.; Schmitt, J.; Decher, G. *Ber. Bunsen.-Ges. Phys. Chem.* **1996**, *100*, 948.
(41) Lösche, M.; Schmitt, J.; Decher, G.; Bouwmann, W. G.; Kjaer, K. *Macromolecules* **1998**, *31*, 8893−8906.
(42) Kovacevic, D.; van der Burgh, S.; de Keizer, A.; Cohen-Stuart, M. A. *Langmuir* **2002**, *18*, 5607−5612.
(43) Fringeli, U. P. Private communication (University of Vienna, 2006).
(44) Righetti, P. G.; Caravaggio, T. *J. Chromatogr.* **1976**, *127*, 1−28.
(45) Levitt, M.; Greer, J. *J. Mol. Biol.* **1977**, *114*, 181−293.
(46) Kabsch, W.; Sander, S. *Biopolymers* **1983**, *22*, 2577−2637.
(47) Koper, G. J. M.; van Duijvenbode, R. C.; Stam, D. D. P. W.; Steuerle, U.; Borkovec, M. *Macromolecules* **2003**, *36*, 2500−2507.
(48) Kodama, H.; Miyajima, T.; Mori, M.; Takahashi, M.; Nishimura, H.; Ishiguro, S. *Colloid Polym. Sci.* **1997**, *275*, 938.
(49) Ladam, G.; Schaad, P.; Voegel, J. C.; Schaaf, P.; Decher, G.; Cuisinier, F. *Langmuir* **2000**, *16*, 1249.
(50) Elliott, A.; Ambrose, E. J. *Nature* **1950**, *165*, 921.
(51) Jackson, M.; Mantsch, H. H. *Crit. Rev. Biochem. Mol. Biol.* **1995**, *30* (2), 95−120.
(52) Woody, R. W. *Biopolymers* **1969**, *8*, 669.
(53) Woody, R. W. In *Peptides, Polypeptides and Proteins*; Blout, E. R., Bovey, F. A., Goodman, M., Lotan, N., Eds.; Wiley: New York, 1974; p 338.
(54) Malinowski, E. R.; Howery, D. G. In *Factor Analysis in Chemistry*; Wiley: New York, 1980.
(55) Chittur, K. K.; Fink, D. J.; Leininger, R. I.; Hutson, T. B. *J. Colloid Interface Sci.* **1986**, *111* (2), 419.
(56) Biesheuvel, P. M.; Van der Veen, M.; Norde, W. *J. Phys. Chem. B* **2005**, *109*, 4172.

BM050631R